

Optomechanical eye model with imaging capabilities for objective evaluation of intraocular lenses

Pier Giorgio Gobbi, PhD, Francesco Fasce, MD, Stefano Bozza, MSc, Rosario Brancato, MD

PURPOSE: To develop an in vitro procedure providing data on the visual performance obtainable with intraocular lenses (IOLs), for objective comparison between IOL models and direct correlation with the relative visual performance attainable in vivo.

SETTING: University Hospital San Raffaele, Milan, Italy.

METHODS: An optomechanical eye model was developed to allow simulated in vivo testing of IOLs. The experimental eye mimics the optics and geometry of the Gullstrand's eye model, with an aspheric poly(methyl methacrylate) cornea, variable pupil, and IOL holder. Its detection system is designed to reproduce the mean resolution of the human fovea. The imaging capabilities of the model eye were measured using monofocal IOLs. The tests included qualitative information, such as appearance of optotype chart images, and quantitative information, such as simulated visual acuity tests for far and near distance at variable contrasts.

RESULTS: Objective numerical IOL evaluation was made possible on the basis of the visual acuity recorded with the eye model. The maximum recorded far acuity for the monofocal IOLs was about 20/14 at full contrast, progressively decreasing for reduced contrast. Best corrected near acuity ranged between 20/14.7 and 20/15.4.

CONCLUSIONS: The optomechanical eye model provided objective grading of IOLs through the evaluation of simulated visual acuity, which can be scaled usefully to human vision. The eye model also allowed the qualitative visualization of IOL imaging properties, making it potentially useful in characterizing and distinguishing different IOL types.

J Cataract Refract Surg 2006; 32:643-651 © 2006 ASCRS and ESCRS

Cataract extraction is the first surgical procedure in the world by number of operations, and consequently pseudo-phakic intraocular lenses (IOLs) are the most diffused prostheses among all implantable medical devices. Today, there is a variety of IOLs according to the lens material (poly[methyl methacrylate] [PMMA], silicone, acrylic), the

optical design (biconvex spherical, aspherical, Fresnel, diffractive, monofocal, bifocal, multifocal), and the optomechanical design (clear optical zone, haptics, thickness, edge shape, accommodative features). Recently, phakic refractive lenses have received increasing attention for refractive surgery procedures.

In such a complex framework, it is difficult for the ophthalmic surgeon to find homogeneous, controlled, quantitative information on IOL properties to help compare and choose among different types with adequate technical support. The only quantitative data available are in the form of modulation transfer function (MTF) plots that manufacturers sometimes include in the IOL technical data sheet, however, without uniformity of test conditions, and, moreover, without a direct link to a sound index for the quality of vision. At the same time, few reports give a comparative optical characterization of some IOLs,¹⁻⁵ and in a few cases

Accepted for publication September 18, 2005.

From Laser Medicine Research, University Hospital San Raffaele (Gobbi, Bozza), and the Department of Ophthalmology and Visual Sciences, University Hospital San Raffaele (Fasce, Brancato), Milan, Italy.

No author has a financial or proprietary interest in any material or method mentioned.

Reprints are not available.

they are limited to an analysis of the optical quality of the lenses.⁶⁻⁹

On the other hand, many clinical studies have evaluated and compared the visual outcomes in large patient populations after lens extraction and IOL implantation. This approach clearly represents an indirect evaluation of the optical properties of an IOL because they are merged in a number of surgical, biological, and individual masking factors, thus requiring hundreds of subjects to reach statistical relevance. This issue gained enhanced interest after the introduction of phakic IOLs used for refractive surgery in demanding patients and of multifocal IOLs because of the unpredictable acceptance of lenses featuring simultaneous imaging from distant and reading distance planes with a net decrease in image contrast and resolution.

The aim of this study was to develop an objective experimental method for the reliable evaluation of the optical properties of IOLs that will provide comparative tests for the behavior of different IOLs using quantitative and qualitative self-explanatory information, easily manageable even without specific optical expertise. The goal was reached through the realization of an imaging optomechanical model of the human eye, reproducing its typical refracting conditions and intended to represent an invariant, well-controlled environment for the optical testing and comparison of different IOLs.

MATERIALS AND METHODS

The Eye Model

The main guideline driving the design of the optomechanical eye model was to reproduce, as closely as possible, the conditions met by an IOL in a real eye. In particular, attention was focused on the following issues:

- *Cornea.* The artificial cornea must account for the mean corneal power of the human eye, providing the proper bending of optic rays onto the IOL.
- *Aqueous humor.* The IOL being tested must be hosted in a liquid environment, resembling the aqueous humor refractive index, at the correct distance from the cornea of an empty capsular bag.
- *Pupil.* A variable iris must mimic the eye's pupil behavior, allowing to vary the IOL numerical aperture.
- *Retina.* The artificial retina must reproduce the human fovea resolution using a convenient image detector.
- *Emmetropia.* The overall eye length must be variable, to accommodate IOLs of different power and to allow accurate focusing of the "retinal" image.

For the optical design, reference was made to Gullstrand's number 1 or "exact" eye model.¹⁰ The model refractive index for the aqueous and vitreous humors, $n_a = 1.336$, was simulated using balanced saline solution (BSS) with index of 1.334. The artificial cornea has to provide about 43 diopters (D) of optical power.¹¹ In practice, no material could be found with a refractive

index as low as the value 1.376 of the Gullstrand's cornea: soft contact lenses lie in the 1.41 to 1.44 range but lack the required stiffness and temporal stability because of dehydration. It was decided to use the well-performing PMMA material ($n = 1.490$), with the same thickness (0.5 mm) and anterior radius of curvature (7.7 mm) of the Gullstrand's model, but changing the posterior radius of curvature to result in 43 D power when in contact with BSS; this implies a calculated value of 7.4 mm in place of the original 6.8 mm.

The cornea was diamond turned by a contact lens crafter (Weis Optics Snc.), with a white-to-white diameter of 10 mm. The anterior surface of the PMMA cornea was given an aspheric prolate shape to reproduce the mean spherical aberration of the human cornea; the mean asphericity value Q of -0.28 ± 0.13 (SD) was taken as reference as topographically measured¹² in a large sample (1030 eyes) of emmetropic subjects with an optic zone of 8 mm. Ray tracing showed that with PMMA, the asphericity producing the same amount of spherical aberration is to be increased to -0.25 , and this was the target asphericity of the design. The posterior surface was maintained as spherical. Corneal topography measurements of the actual PMMA cornea resulted in a mean power of 43.50 D with an asphericity of -0.30 (5 mm zone).

Behind the PMMA cornea, a stainless steel disk punched with different aperture holes provided pupils with sizes 2, 3, 4, 5, 6, and 8 mm. The disk was pivoted eccentrically to the optical axis and could be turned from outside the eye mount; its axial position resulted in an anterior chamber depth (distance of the rear plane of the pupil disk from the posterior corneal surface; Figure 1) of 3.1 mm. The pupil size seen from outside the eye model is magnified by the cornea-aqueous combination by a factor of about 1.13; this larger image represents the entrance pupil of the system and is the significant quantity for human eyes because it is the only measurable aperture size. The IOL was held in place by 2 metal rings that clamped the IOL haptics, attached to a mount which allowed a fine axial translation of ± 2 mm around the mean position. The proper location for the IOL was chosen to correspond to the space (1 mm thick) between the principal planes of the unaccommodated lens in the Gullstrand eye model; namely, 1.56 mm after the anterior pole surface and 1.04 mm before the posterior pole surface.

To detect the image formed by the model eye, the most obvious substitute of the human retina appears to be a color charge-coupled device (CCD) image sensor. However, assuming a cone density in the fovea of $180\,000\text{ mm}^{-2}$ (Oyster¹³) and a square matrix arrangement, the center to center spacing between adjacent cones is about $2.4\ \mu\text{m}$. In comparison, a one-third inch CCD camera with a $3.3\text{ mm} \times 4.4\text{ mm}$ sensor, has single pixels of $5.67\ \mu\text{m} \times 5.85\ \mu\text{m}$ (PAL standard); that is, the linear spacing is 2.44 times larger than in the human fovea. To bring the CCD-resolving capability to the same level of the fovea, an optical magnification of the "retinal" image by a factor of 2.44 is necessary.

Thus, in the optomechanical eye, the primary image (formed by cornea, IOL, and BSS) was focused on a glass window. Then, an optical relay was made out of the model eye, coupling the primary retinal image to the CCD plane with the desired magnification (Figure 1). To this end, 2 television objectives were used: a zoom 12.5 mm to 75 mm, 1:1.2, and a 16 mm, 1:1.4 (Computar); the 2 lenses were coupled front to front focused at infinity. The zoom lens was tightened to the CCD mount, and the zoom varied until the desired magnification was reached. The lens plate, acting as an ocular fundus, bore a graduated reticle on its inner surface, which served a double purpose: to allow precise focusing of the relay optics on the window surface (Figure 1) and to introduce

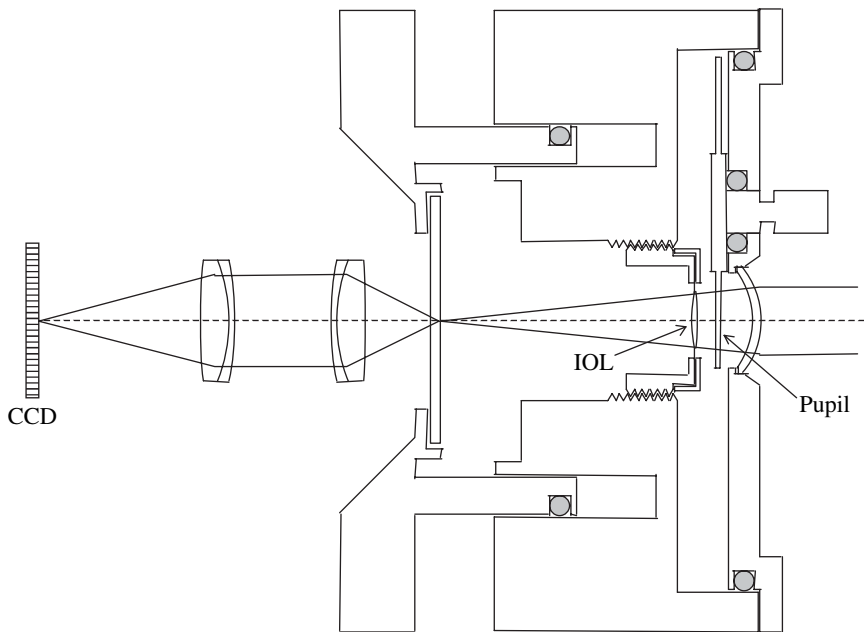


Figure 1. Optical and mechanical schematic layout of the experimental model eye.

an absolute length reference in the resulting image, used to calibrate exactly the relay magnification and to size the image itself.

The eye model components (cornea, iris, IOL mount, and retina) were assembled into a watertight aluminum structure (Figure 2, A) with its internal surfaces blackened to reduce stray light. The overall axial length (distance from corneal apex to retina) could be varied micrometrically between 20 mm and 30 mm, allowing it to host high-power IOLs as well as to simulate an aphakic eye. The television camera (a single-chip color analog CCD) was mounted on a micrometric translation stage (Figure 2, B). The CCD output signal was displayed on a television monitor and recorded on a digital tape for further analysis. Operatively, the CCD camera was first moved to give a sharp image of the reticle grooved on the inner surface of the glass retina. Then, the eye model length was tuned to look for the best television image of the external scene. No color filter was added to the optical system.

Intraocular Lenses

Two monofocal IOL models were used to exploit the overall performance of the optomechanical eye model: the Alcon AcrySof MA60BM, a biconvex acrylate IOL with square-edged posterior surface design, and Alcon AcrySof Natural SN60AT, an asymmetric biconvex IOL of ultraviolet-absorbing acrylate/methacrylate copolymer, with a yellow appearance. Both IOL samples had the same nominal power (21.0 D).

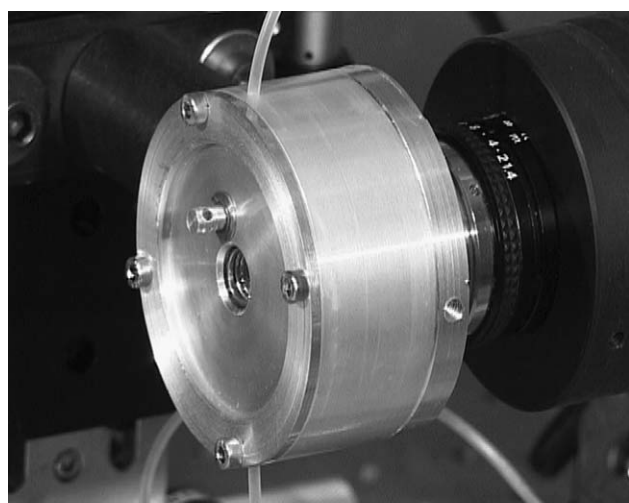
Psycho-Physical Tests

The optomechanical eye model was used to simulate psycho-physical tests usually performed on humans, such as visual acuity and contrast sensitivity tests at far and near. Two types of data were taken: digitized samples of the TV image produced by the CCD camera as well as readings given by a masked subject (P.G.G.) looking at the same image and asked to identify letters on visual acuity charts and grating orientation in contrast sensitivity

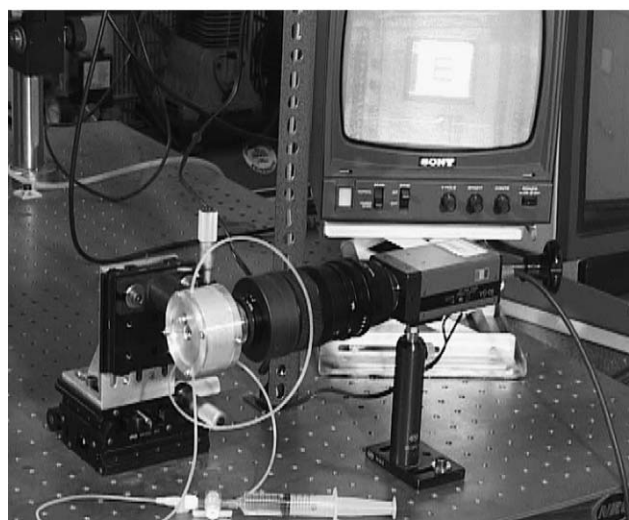
patterns. In a first demonstration trial,¹⁴ common optotype charts such as the Early Treatment of Diabetic Retinopathy Study (ETDRS)¹⁵ letter chart and Functional Acuity Contrast Test (FACT) sine-wave grating chart were used.¹⁶ However, this approach could not be applied to iterative multiple testing because of the bias in the test outcome induced by memorization effects developed in the masked reader.

It was thus decided to make use of ETDRS characters generated by a computer and displayed on a monitor in random sequences. At the same time, because of the low test-retest reliability of contrast sensitivity measurements using sine-wave gratings with forced-choice procedure,¹⁷ contrast sensitivity was evaluated using low-contrast versions of the same ETDRS set of letters, a technique with an inherently much higher reliability (0.98 versus 0.77).^{18,19} This type of test was named contrast acuity to distinguish it from conventional contrast sensitivity tests.²⁰ Using a Millennium G 450 graphics card (Matrox Graphics Inc.) mounted in a personal computer (PC), it was possible to generate characters with contrast continuously variable from 100% to 2%; with a 15-inch cathode ray tube monitor, the allowed character size at 6 m distance could range from logMAR -0.3 (Snellen 20/10) up to logMAR $+1.3$ (Snellen 20/400). The characters used were the 10 Sloan letters²¹ grouped in the 28 combinations of 5 letters that the ETDRS recognized as having nearly the same intermediate difficulty score.²² For each visual acuity line at any contrast, an entire 5-letter group was used, randomly chosen among the 28, with letters displayed on the cathode ray tube monitor 1 at a time, in random sequence within the group itself (Figure 3, A).

All the operations of displaying the characters and checking the reader response were automatically managed by the PC (the relative ad hoc software was written in Visual Basic). In practice, the reader had to first input the contrast level and the starting visual acuity level of the ongoing test and then hit on the keyboard the letter identified by looking at the eye model image displayed on the television monitor (Figure 3, B). The reader was masked in that he could not see the letter actually prompted by the PC



A



B

Figure 2. A: Close view of the model eye assembly. B: Experimental setup.

monitor. For each successfully recognized letter, 0.02 was subtracted from the overall logMAR score, and for each failure the score did not change. The test stopped when no character in a visual acuity line was recognized correctly. The final logMAR score represented the visual acuity performance of the test. For each IOL, visual acuity was measured at 6 contrast values: 100%, 50%, 20%, 10%, 5%, and 2%, and 2 pupil sizes: 3 and 5 mm. At every condition, the visual acuity measurements were repeated 3 times.

As stated, these far distance visual acuity tests were performed with the PC monitor placed 6 m from the eye model cornea. Exactly the same measurements were repeated at 40 cm as reading distance visual acuity tests. This was accomplished without altering the operative conditions through the insertion of an optical relay in the path from the cornea to the PC monitor, which realized a conjugation of the 6 m plane to the 40 cm plane, together with an optical magnification of 1/15. The required 3.1 D relay optics was obtained with the combination of 2

cemented doublets of +5 D and -4 D powers separated by 105 mm (Figure 4). In this way, switching from far to near distance testing was easy and fast, requiring no adjustments, and both tests were measured in identical calibrated conditions and reported with the same measurement units.

All visual acuity values, for both far and near distance, are reported in logMAR units; the minimum angle of resolution (MAR) is given by the angular width (expressed in minutes of arc) of the limb of the smallest letter recognized at 6 m distance. Thus, $VA_{\log\text{MAR}} = \log_{10}(\text{MAR})$, where VA is visual acuity. Conversion into decimal notation is obtained through $VA_D = 1/\text{MAR}$, whereas the Snellen fraction notation at 20 feet distance is given by $VA_{\text{SF}} = 20/(20 \times \text{MAR})$.

RESULTS

Chart Test

Figure 5, B, visually depicts the imaging performances of the optomechanical eye model, showing the digitized electronic record of the retinal image corresponding to the projection of the ETDRS chart of Figure 5, A (far distance, MA60BM IOL). The graduated reticle of Figure 5, B, has a tick spacing of 0.1 mm. The superimposed white broken circle represents the equivalent size of the foveola (1 degree \sim 0.3 mm), and the black solid circle corresponds to the fovea edge (5 degrees \sim 1.5 mm), where human visual acuity is estimated to be about 50% and 25% of the peak center value, respectively.

Contrast Acuity Test

The mean numerical outcomes of the quantitative far visual acuity tests performed at various letter contrasts with the 2 monofocal IOLs are reported (mean value \pm SD) in Figure 6 for 5 mm pupil size. The corresponding curves for near distance visual acuity are given in Figure 7 and are taken with an additional lens of +2.875 D placed 12 mm from the corneal apex, experimentally chosen for the sharpest imaging at 40 cm; the data in Figure 7 are thus better referred to as best corrected visual acuities (BCVAs).

Globally, the contrast acuity differences between the 2 IOLs are not significant, although borderline: $P < .0222$, $F_{1,4} = 13.16$; in this case, the significance threshold had to be lowered at the 0.01 level owing to the multiple-comparison (Bonferroni) correction. The behaviors at 3 mm pupil size almost exactly overlap the curves at 5 mm and are not reported.

DISCUSSION

The quality of vision obtainable after IOL implantation is a primary issue, with relevant technical, clinical, and commercial implications. Recently, attempts were made to not only improve the safety, biocompatibility, clarity, and ease of insertion of IOLs, but also to enhance the

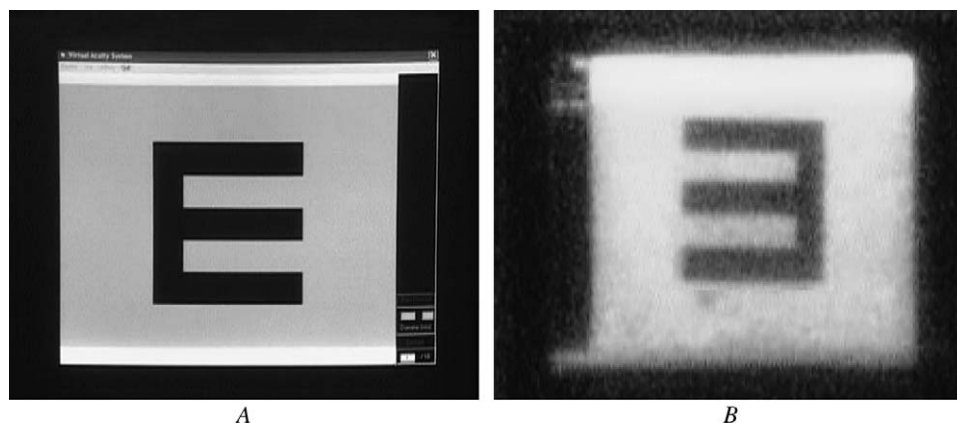


Figure 3. Pictures of the computer-generated Albin's "E" prompted by the PC monitor (A) and of its retinal image displayed on the TV monitor (B). The image is inverted up-down and left-right, as in a real eye.

expected visual performance through material choice and sophisticated optical design. Being able to measure the effects induced by different IOL models on human vision in a rigorous, quantitative, but handy way would result in a considerable advantage.

In a recent study,⁴ an artificial eye model, built according to the Gullstrand simplified schematic eye, was used to measure the point spread function (PSF) of multifocal and monofocal IOLs. The comparison was carried on through the evaluation of the MTF and Strehl ratio, and no attempt was made to translate the results from the optical to the psychophysical language.

Modulation transfer function was also evaluated⁵ in a set of 24 different monofocal IOLs after recording the line spread function produced by each implant suspended

in air and without simulation of the corneal power, in an optical test bench. The study was limited to the analysis of the passband spatial frequency (corresponding to the point at -3 dB, or 71%, of the low-frequency modulation transfer).

However, converting the technical information associated with the knowledge of MTF into manageable clinical information, such as visual acuity or contrast sensitivity, requires introduction of a proper model of the human retinal response, particularly the contrast threshold function. This procedure is not straightforward or univocal, but it can lead to significant, although gross, insights into the expected changes in visual performance from the comparison of a multifocal and a monofocal IOL.²³

We followed a different approach to characterize the imaging properties of IOLs. The optomechanical model we describe is anatomically accurate in that it faithfully reproduces sizes, spacings, and optical powers of the human eye. Contrary to the experimental setup recommended^{24,25} to evaluate IOL resolution and MTF (eye cells), where the corneal power is produced by an aberration-optimized, achromatic optic external to the IOL cell,^{9,26-29} in our case, the PMMA cornea was designed, to reproduce not only the actual mean corneal power, but also the external curvature, thickness, spacing from pupil and IOL, and spherical aberration. Also chromatic aberration is expected to be equivalent to that of a real eye because of the similar constringence of PMMA and corneal stroma (57.2 and 56, respectively). Incidentally, the PMMA cornea of the artificial eye developed by Pieh et al.,⁴ exactly reproducing the curvatures of the Gullstrand eye model, has a power in defect by 4% relative to the Gullstrand power as a result of the different refractive index.

This optical affinity allowed us to evaluate and compare IOL imaging performances in an optical setup similar to the in vivo arrangement (the major optical feature missing in the model eye being an apodized pupil reproducing the

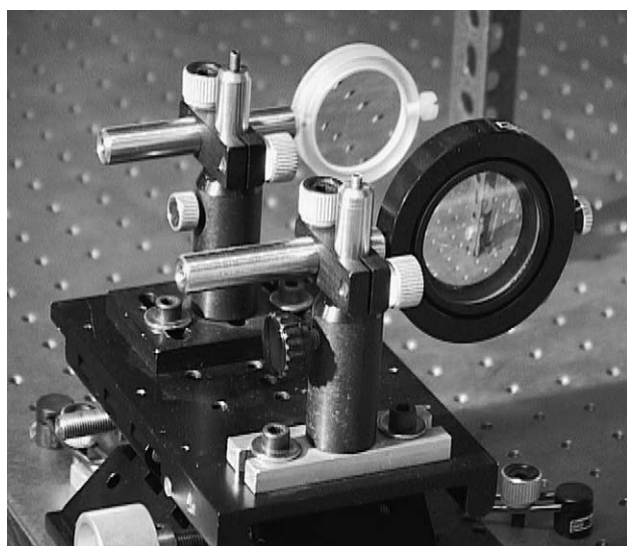
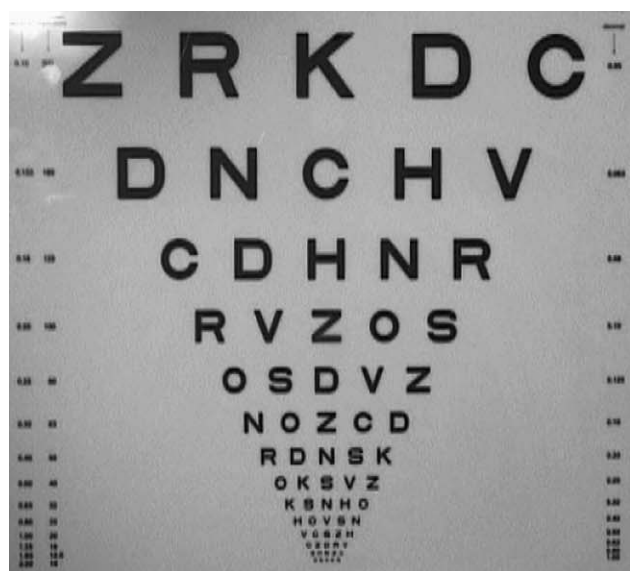
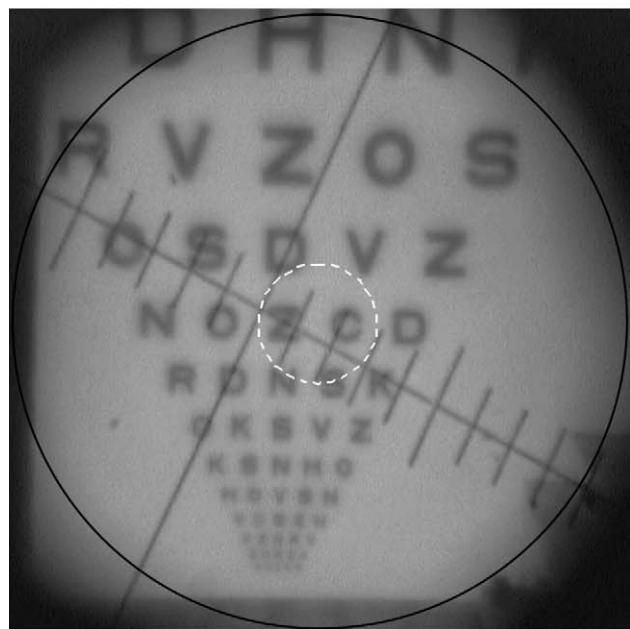


Figure 4. The relay optics used to conjugate the far distance plane (6 m) with the near distance plane (40 cm).



A



B

Figure 5. A: The ETDRS optotype chart. B: Image of A seen by the eye model (distance 6 m, IOL MA60BM, pupil 5 mm). The reticle tick spacing on the retina is 0.1 mm. The white and black circles correspond to the approximate edges for foveola and fovea, respectively.

Stiles-Crawford effect), overcoming the difficulties of comparison of frequency-response measurements performed in different experimental arrangements and of direct comparison with clinical measurements. As a result, the retinal image is expected to carry the signature of spherical and chromatic aberrations of both IOL and artificial cornea. This image can then be analyzed with standard optical

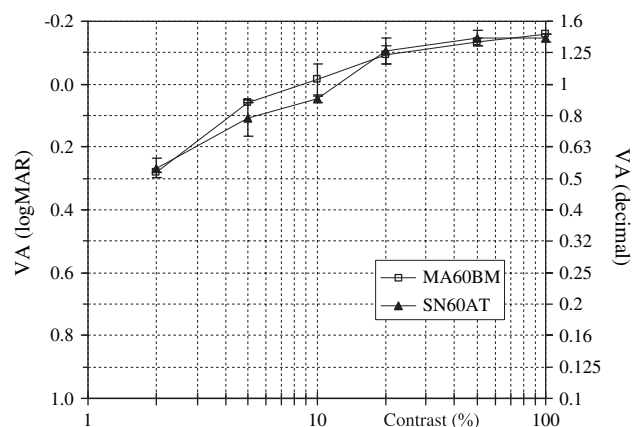


Figure 6. Plot of visual acuity versus letter contrast at far distance (6 m) with 5 mm pupil size (VA = visual acuity).

methods to recover PSF, MTF, or aberration coefficients for different pupil sizes, as done in other studies.^{1,2,4,5,8,30} All these quantities completely characterize the linear optical behavior of the eye model, thus allowing immediate and homogeneous comparison of IOLs with equal dioptric power and different material or design features.

Such a characterization, although detailed and exhaustive, is of little help to anyone who is not well acquainted with the technical language of physical optics and aberrometry. More important, as noted, such quantities are not easily related to a single quantitative index of vision quality. Because ophthalmologists are used to measure the level of visual performance in terms of visual acuity and contrast sensitivity, a more familiar and handy evaluation of the IOL performance would result if just these psychophysical vision tests could be performed using the model eye.

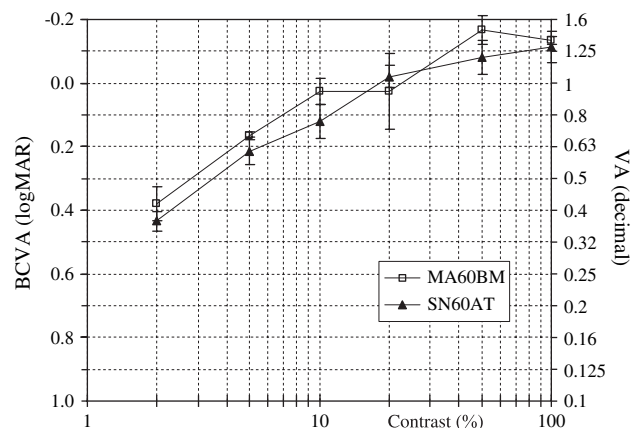


Figure 7. Plot of BCVA versus letter contrast at near distance (0.4 m) at a 5 mm pupil with an additional lens of 2.875 D (VA = visual acuity).

The optical resolution of the final television image obtained with the current eye model is comparable to that occurring through foveal sampling in a real human eye. In other words, both optics and image sampling are similar in the 2 cases. What cannot be reproduced, of course, is the detection process (ie, sensitivity, dynamic range, nonlinearity, noise) and the image elaboration (retinal and cortical processing are excluded). However, most features of the brain's skill to identify patterns and shapes are reintroduced if a subject is asked to recognize and read optotype characters of variable size and contrast, "seen" by the model eye and displayed on a television monitor, or analogously to guess the orientation of sinusoidal patterns of variable spatial frequency and contrast. In this way, the subjective visual performance of the reader is not involved in the procedure because of the electronic image magnification. The result is objective, quantitative data from simulated psychophysical tests aimed at measuring visual acuity (distance and near) and contrast sensitivity in the form of threshold visual acuity values as a function of pupil size, or threshold contrast values versus spatial frequency. If different IOLs are tested in this way under identical conditions (same characters, illumination, and analyzing subject), the data obtained are directly related to the optical (and visual) performance offered by each IOL. Thus, a quantitative comparison can be easily established.

Specifically, the results of the tests on the 2 monofocal IOLs in Figures 6 and 7 indicate that the presence of the UV-absorbing yellow pigment in the SN40AT IOL does not alter the obtainable visual performance at a significant level relative to the MA60BM.

In the current study, we report only contrast acuity tests. We also performed a few trials of contrast sensitivity evaluations using sinusoidal patterns of variable contrast and spatial frequency; however, the measurements turned out to be exceedingly erratic in test–retest repeatability, thus requiring many iterations of the run for each tested condition. The process was also lengthy, especially when adopting the 2-alternative, forced-choice method together with the "staircase" thresholding procedure. This struggle between accuracy and efficiency is an inherent, unresolved drawback of all contrast sensitivity tests,³¹ and we preferred to base our analysis on the more reliable contrast acuity tests only.

The reliability of the procedure was explored further by repeating both contrast acuity and contrast sensitivity tests in constant conditions but with different readers. The variability in the final results was of the same order of the test–retest variation observed with the same reader for the contrast acuity test, whereas for contrast sensitivity test, it was much higher than the already large spread seen in repeated trials with the same reader. The observed

overlap of intersubject contrast acuity readings clearly indicates that the subjective influence of the reader on the measurement outcome is marginal, thus outlining the objectiveness of the procedure, whereas the spread of intra-subject data is only the result of the intrinsic fluctuation in letter recognition at the visibility limit because of forced guessing. By increasing the number of repeated tests, the data spread is expected to progressively reduce, thus possibly allowing even tiny differences in visual performance to be appreciated among IOLs.

The procedure we present is to be compared with the ordinary clinical practice of IOL evaluation through *in vivo* subjective testing; in these cases, every data point corresponds to a single visual acuity measurement performed in an implanted eye, usually at full contrast, and is affected by a number of variability factors that are surgical (tilt, decentration, residual refractive error, induced astigmatism), biological (corneal and vitreous transparency, pupil size, foveolar response, neuronal integrity), and individual (subject collaboration, test endpoint, measurement accuracy, environmental conditions). To eliminate such a pronounced variability and to reach a degree of "objectiveness" comparable to that seen in our approach, a large amount of eyes and time would be required, very likely at an unpractical level. Moreover, it would be without the benefit of discriminating visual performance against letter contrast and pupil size.

It is worth commenting briefly on the observed insensitivity of contrast acuity measurements to pupil size. One would expect the visual performance to be degraded when passing from a 3 mm to 5 mm pupil because of stronger spherical aberration. Although no effort was made to refine the discrimination between the 2 pupil sizes, such an outcome could be explained partially by a couple of factors related to our eye model structure. The first is represented by the corneal asphericity, which was measured to be smaller than designed (-0.30 versus -0.25). Even if its value is far from nulling the spherical aberration of the PMMA cornea (which occurs for $Q = -0.55$), the small deviation in Q acts in the direction of underestimating the overall spherical aberration. The second factor is related to the presence of an automatic adjustment of the mean irradiance on the CCD camera (automatic gain control [AGC]). This feature has no effect on the measurements performed at constant pupil size because the overall irradiance of the PC monitor is maintained constant for any value of contrast. However, switching to a larger pupil results in an increase in the luminous flux on the CCD, hence, in a lower gain by the AGC and lower noise in the displayed CCD image. The effect cannot be quantified, but again, although minimal, it tends to enhance the visual performance at larger pupils.

Visual acuity measurement obtained with low-contrast letters does not translate directly into ordinary plots of the

contrast sensitivity function (contrast sensitivity versus spatial frequency) unless the heuristic assumption is made that threshold letter identification requires 2.5 cycles per letter.^{16,32} One such contrast sensitivity function plot is shown in Figure 8, relative to far distance; basically, it is the same plot as in Figure 6, rotated clockwise by 90 degrees and with a double rescaling of axes. Such a reconstruction cannot reach contrast sensitivity values greater than 50 for technical limitations (because of the PC graphics card and monitor) and cannot equally cover the low-frequency region (<3 cycles per degree) for letter-size limitations. The curves of Figure 8 clearly resemble the trailing tails of ordinary contrast sensitivity function curves obtained with projection of sinusoidal gratings. However, the plots in Figure 8 have 2 pitfalls: the arbitrariness involved in assigning equivalent periodic frequencies to a-periodic characters and the different triggering mechanism of the visual perception channels by sine-wave gratings and alphabetic characters.³³

Little can be inferred from the absolute level reached in the above IOL test, for instance from the distance visual acuity level measured in specific conditions. However, differences in visual acuity levels observed with different IOLs under identical ambient conditions or with the same IOL but different pupil sizes are meaningful and representative of differences in visual acuity directly transferable to human visual perception. The same applies to reading distance visual acuity tests. In fact, the entire picture can be modeled by assuming that the level of visual acuity measured with the model eye; for instance VA_M is proportional to the level attainable in "live" conditions; that is, in a real "mean" eye, for instance VA_L , through a proportionality constant:

$VA_M = \alpha \times VA_L$. The scale factor α includes the differences in image detection and processing between the model and a real eye, described above. Denoting with apex 1 and 2 the data relative to 2 different conditions (eg, different IOLs), it follows: $VA_M^1 = \alpha \cdot VA_L^1$ and $VA_M^2 = \alpha \cdot VA_L^2$, hence $\frac{VA_M^1}{VA_M^2} = \frac{VA_L^1}{VA_L^2}$; that is, the ratio of performances is equal for the model eye and for the real eye. Because visual performances (both visual acuity and contrast sensitivity) are measured on logarithmic scales, it follows that differences of logarithmic values (for visual acuity, logMAR or visual acuity line differences) are maintained in the model and the real eye. In other words, the plots in Figures 6 and 7 are to be seen as applicable to real subjects, reflecting performance differences of individual IOLs, apart from possible shifts in the vertical visual acuity scale. Of course, these data were taken in well-controlled conditions with constant luminance and fixed pupil size.

From the results shown, it can also be inferred that the factor α above is indeed not far from unity; that is, the resolving capability of the model eye is likely within 1 or 2 visual acuity lines from the mean human behavior. To this end, the far distance performances of the IOLs at full contrast (Figure 6) can be taken as a paradigm: The mean VA levels recorded at full contrast were -0.16 logMAR (1.45 decimal, 20/13.8 Snellen fraction) for the MA60BM IOL and -0.147 logMAR (1.4 decimal, 20/14.3 Snellen fraction) for the SN60AT IOL. These values confirm that the optomechanical eye model performances are definitely better than the conventional mean human performance of 0 logMAR by 1.5 visual acuity lines, well within the range of values observed in an emmetropic population.

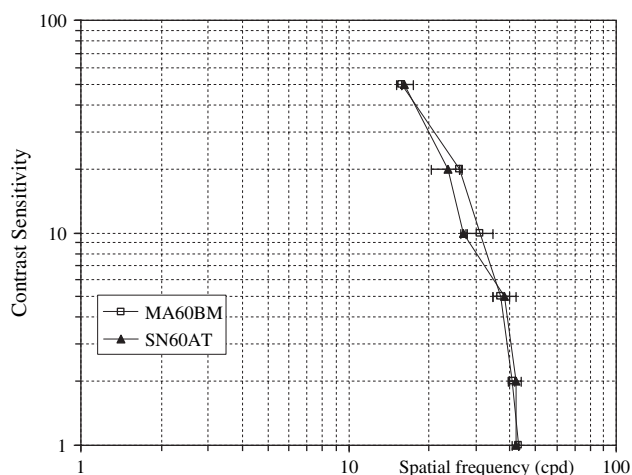


Figure 8. Contrast sensitivity function at far distance, 5 mm pupil size, derived from the visual acuity measurements of Figure 6 (cpd = cycles per degree).

CONCLUSION

We developed a method to obtain reliable, quantitative information about the imaging performances of IOLs of any type. The procedure is based on use of an experimental eye model that reproduces the refracting and detecting conditions usually met in a mean human eye and represents the test bench for the comparison of different IOL models or even IOL types. The test outcome is given by quantitative descriptors of the quality of image realized with the experimental eye, such as aberrometry or point spread function, or by more handy metrics such as visual acuity and contrast sensitivity scores retrieved from simulated visual acuity and contrast sensitivity measurements at far and near distance by a masked reader interpreting the electronic image produced by the model eye.

Also, the qualitative information that can be obtained with the model eye—typically the appearance records of standardized images—can be useful to illustrate the specific features of different IOLs and to help in the relative

comparison process for both vision research and routine clinical applications.

REFERENCES

- Holladay JT, van Dijk H, Lang A, et al. Optical performance of multifocal intraocular lenses. *J Cataract Refract Surg* 1990; 16:413–422; erratum, 781
- Knorz MC, Lang A, Hsia T-C, et al. Comparison of the optical and visual quality of poly(methyl methacrylate) and silicone intraocular lenses. *J Cataract Refract Surg* 1993; 19:766–771
- Williamson W, Poirier L, Coulon P, Verin P. Compared optical performances of multifocal and monofocal intraocular lenses (contrast sensitivity and dynamic visual acuity). *Br J Ophthalmol* 1994; 78:249–251
- Pieh S, Marvan P, Lackner B, et al. Quantitative performance of bifocal and multifocal intraocular lenses in a model eye; point spread function in multifocal intraocular lenses. *Arch Ophthalmol* 2002; 120:23–28
- Tognetto D, Sanguinetti G, Sirotti P, et al. Analysis of the optical quality of intraocular lenses. *Invest Ophthalmol Vis Sci* 2004; 45:2682–2690
- Grossman LW, Igel DA, Faaland RW. Survey of the optical quality of intraocular lens implants. *J Cataract Refract Surg* 1991; 17:168–174
- Faaland RW, Grossman LW, Igel DA. Optical quality testing of monofocal intraocular lens implants with a 3 mm and a 4 mm aperture. *J Cataract Refract Surg* 1991; 17:485–490
- Christie B, Nordan L, Chipman R, Gupta A. Optical performance of an aspheric multifocal intraocular lens. *J Cataract Refract Surg* 1991; 17:583–591
- Simpson MJ. Optical quality of intraocular lenses. *J Cataract Refract Surg* 1992; 18:86–94
- Gullstrand A. The optical system of the eye. In: Southall JPC, ed, *Helmholtz's Treatise on Physiological Optics*, translated from the third German edition, Vol I. Rochester, NY, Optical Society of America, 1924; Appendix II.3, 350–358
- Gobbi PG, Carones F, Brancato R. Keratometric index, videokeratography, and refractive surgery. *J Cataract Refract Surg* 1998; 24:202–211
- Calossi A. The optical quality of the cornea. In: Caimi F, Brancato R, eds, *The Aberrometers; Theory, Clinical, and Surgical Applications*. Canelli, Italy, Fabiano Editore, 2003; 133–162
- Oyster CW. *The Human Eye; Structure and Function*. Sunderland, MA, Sinauer Associates, 1999
- Gobbi PG, Fasce F, Bozza S, Brancato R. Experimental characterization of the imaging properties of multifocal intraocular lenses. In: Manns F, Söderberg PG, Ho A, eds, *Ophthalmic Technologies XIII*, SPIE Proc 2003; 4951:104–111
- Ferris FL III, Kassoff A, Bresnick GH, Bailey I. New visual acuity charts for clinical research. *Am J Ophthalmol* 1982; 94:91–96
- Ginsburg AP. Next generation contrast sensitivity testing. In: Rosenthal BP, Cole RG, eds, *Functional Assessment of Low Vision*. St Louis, MO, Mosby, 1996; 77–88
- Rubin GS. Reliability and sensitivity of clinical contrast sensitivity tests. *Clin Vis Sci* 1987/88; 2:169–177
- Pelli DG, Robson JG, Wilkins AJ. The design of a new letter chart for measuring contrast sensitivity. *Clin Vis Sci* 1997/88; 2:187–199
- Lempert P. Standards for contrast acuity/sensitivity and glare testing. In: Nadler MP, Miller D, Nadler DJ, eds, *Glare and Contrast Sensitivity for Clinicians*. New York, NY, Springer-Verlag, 1990; 113–119
- Knorz MC, Koch DD, Martinez-Franco C, Lorger CV. Effect of pupil size and astigmatism on contrast acuity with monofocal and bifocal intraocular lenses. *J Cataract Refract Surg* 1994; 20:26–33
- Sloan LL, Rowland WM, Altman A. Comparison of three types of test target for the measurement of visual acuity. *Q Rev Ophthalmol* 1952; 8:4–16
- Ferris FL III, Freidlin V, Kassoff A, et al. Relative letter and position difficulty on visual acuity charts from the Early Treatment Diabetic Retinopathy Study. *Am J Ophthalmol* 1993; 116:735–740
- Lang A, Portney V. Interpreting multifocal intraocular lens modulation transfer functions. *J Cataract Refract Surg* 1993; 19:505–512
- ISO 11979-2. *Ophthalmic Implants—Intraocular Lenses—Part 2: Optical Properties and Test Methods*. Geneva, International Organization for Standardization, 1999
- American National Standard for Ophthalmics—Intraocular Lenses—Optical and Physical Requirements. New York, NY, American National Standards Institute, 2002; ANSI Z80.7–2002
- Holladay JT, Ting AC, Koester CJ, et al. Intraocular lens resolution in air and water. *J Cataract Refract Surg* 1987; 13:511–517
- Grossman LW, Knight WB. Resolution testing of intraocular lenses. *J Cataract Refract Surg* 1991; 17:84–90
- Portney V. Optical testing and inspection methodology for modern intraocular lenses. *J Cataract Refract Surg* 1992; 18:607–613
- Norrby NES, Grossman LW, Geraghty EP, et al. Determining the imaging quality of intraocular lenses. *J Cataract Refract Surg* 1998; 24: 703–714
- Peli E, Lang A. Appearance of images through a multifocal intraocular lens. *J Opt Soc Am A* 2001; 18:302–309
- Wolfe JM. An introduction to contrast sensitivity testing. In: Nadler MP, Miller D, Nadler DJ, eds, *Glare and Contrast Sensitivity for Clinicians*. New York, NY, Springer-Verlag, 19; 5–23
- Smith G, Atchison DA. *The Eye and Visual Optical Instruments*. Cambridge, Cambridge University Press, 1997
- Ginsburg AP. Spatial filtering and visual form perception. In: Boff KR, Kaufman L, Thomas JP, eds, *Handbook of Perception and Human Performance*, Vol 2. New York, NY, John Wiley & Sons, 1986 (chap 34)